STUDY ON CALIBRATION DATA PROCESSING OF LARGE APERTURE MICROWAVE RADIOMETER

Zhenhua ZHU[1], Teer BA[2]*, Jun JIANG[3], Yingting FAN[4], Yijin LIANG[5]

Spaceborne microwave radiometer, as the most important passive microwave remote sensing instrument, plays a significant role on the on-orbit exploration satellites, such as FengYun-3 meteorological, HaiYang-2, and the Change lunar satellite. However, at present, the microwave radiometer in orbit is mainly loaded on polar orbiting satellites. The geostationary microwave radiometer has not been realized and applied. In this paper, a segmented calibration method is proposed to improve the on-orbit calibration accuracy of geostationary orbit microwave radiometer. The curve fitting accuracy in the calibration process is effectively improved when the processing of remote sensing data reaches up to a certain quantitative level. In the process of parameter estimation, the least square method is used to improve the estimation accuracy. The new calibration method is compared with the classical linear and quadratic model calibration schemes. The analysis results of the calibration data of the geostationary microwave radiometer show that the segmented calibration scheme significantly improves the precision and accuracy for later product generation and numerical weather prediction.

Keywords: Calibration, Feed interface, Antenna interface, Calibration accuracy, Accuracy

1. Introduction

The spaceborne microwave radiometer is a significant remote sensing detector for meteorological satellites and marine satellites [1]. The radiometer is primarily used for atmospheric, oceanic, terrestrial, and celestial microwave remote sensing. Spaceborne microwave remote sensing is the most important remote sensing technique in meteorology, oceanic, and disaster monitoring. This radiometer can continuously and autonomously monitor global meteorological and oceanic parameters, such as water vapor content, rainfall, sea surface temperature, etc., under nearly all-weather conditions. These features allow for medium and long-term weather forecasts with improved forecast accuracy and real-time and continuous oceanic monitoring.

[1]The first author, Doctoral candidate, National Mobile Communications Research Laboratory, Southeast University, e-mail: zzhsteed@163.com
[2] Communication author, Associate Professor, National Mobile Communications Research Laboratory, Southeast University, e-mail: bateer@seu.edu.cn
[3] Engineer, Shanghai Institute of Satellite Engineering, e-mail: 591718053@qq.com
[4] Engineer, Shanghai Institute of Satellite Engineering, e-mail: fanyingting_sh@163.com
[5] Engineer, Shanghai Institute of Satellite Engineering, e-mail: laofly86128@163.com

A microwave radiometer is a passive remote sensing instrument used to measure the microwave radiation energy of a target. The microwave radiation signal of the target is a weak incoherent signal. The power of the signal is much lower than the power of the radiometer noise. The radiometer itself is a receiver with high sensitivity. Whether the microwave radiometer can obtain valuable sensing data in orbit and achieve quantitative applications and services mainly depends on the calibration accuracy of the microwave radiometer [2-4].

Many studies on the calibration of microwave radiometers have been carried out. Dawei An et al. of the Chinese Meteorological Administration proposed a two-point linear calibration correction + cubic equation nonlinear modeling correction method [5] for the on-orbit nonlinear calibration of the microwave thermometer of the Fengyun No. 3 meteorological satellite. Good calibration and correction of the deviation of the nonlinear characteristics of the thermometer could be obtained using their method. Weiying Chen et al. at the Shanghai Aerospace Electronic Technology Institute studied the nonlinear deviation of the microwave imager on Fengyun-3 [6]. Other research institutes also reported studies related to the on-orbit calibration accuracy of the microwave radiometers.

This study investigated the on-orbit calibration accuracy of large-aperture microwave radiometers in geostationary orbit [7]. Different from the microwave radiometers carried by Fengyun- 3 [8] and Chang'e-1 satellites and the Shenzhou spacecraft, the geostationary orbit microwave radiometer uses a large aperture scheme [9] using the antenna + feed interface calibration scheme [10]. This study examined the nonlinear model for the effective calibration of the large- aperture microwave radiometer. This calibration method with higher-order curve characteristics could improve the microwave calibration.

First, a model of the system based on the characteristics of the geostationary orbit microwave radiometer was established. Second, a piecewise linear calibration model and the corresponding parameter estimation method were proposed. Then the ground calibration data were used for estimation. The results confirm a significant improvement in the accuracy using our calibration method.

2. System Model

The large-aperture microwave radiometer is composed of an antenna, calibration components, feed network, receiver, etc. [11] as shown in Fig 1. The geostationary orbit microwave radiometer consists of six parts: the information processing component, thermal controller, antenna, calibration component, quasi-optical feed network, and receiver.

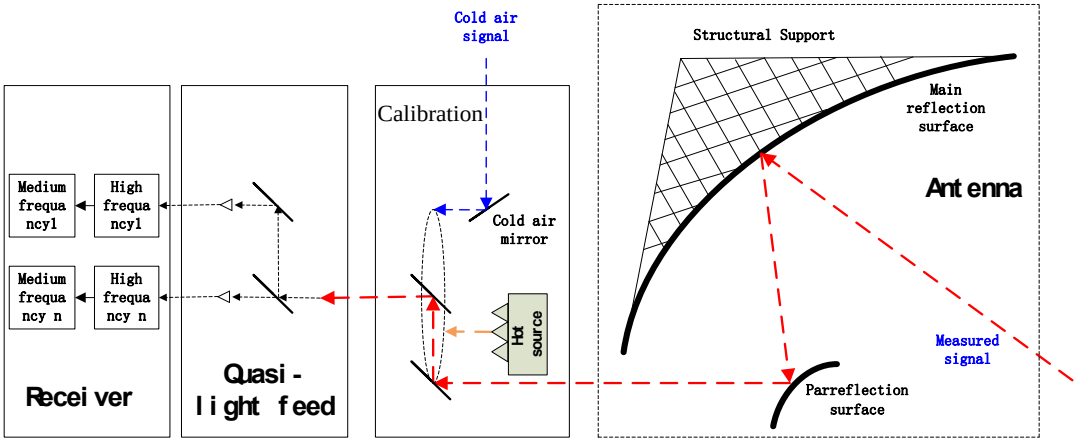

Fig 1: Schematic diagram of the large-aperture microwave radiometer components.

The microwave radiometer signals, including cold signal, hot calibration source signal, and the signal reflected by the antenna that needs to be measured, enter the receiver from the feed interface periodically for measurement. Two main processes are involved: rotating calibration + feeding + receiving and large-aperture antenna reflection.

2.1 System Model

In the calibration process, based on Planck's radiation law [12], and using the Rayleigh-Jones approximation, including the concept of non-ideal black body radiation, the relationship between power and temperature in radiometry is obtained as follows:

$$P = 2kT_B\Delta f \tag{1}$$

where P is the power, k is the Boltzmann constant, T_B is the brightness temperature, and Δf is the receiver bandwidth.

Equation 1 assumes that there is a linear relationship between the power received by the radiometer receiver and the brightness temperature of the observed target in passive microwave remote sensing. Two steps are required to establish the receiver transfer function. First, a variable brightness temperature source with a known brightness temperature T_B was placed on the antenna or feed interface. The output voltage is linear relative to the known brightness temperature. It is sufficient to only measure the corresponding V_O values of two different T_B values for calibration. This method is called a two-point calibration. The calibration equation is as follows:

$$T_B = a \times V_O + b \tag{2}$$

where a and b are the calibration coefficients of the microwave radiometer.

According to the principle of "two points define a straight line" [13], and as long as two inputs of known brightness temperatures are provided, the relationship between the output voltage of the microwave radiometer and the input brightness temperature can be determined according to their output. The constants and the linear equation were determined. For the spaceborne radiometer applications, the low-temperature reference is the cosmic background radiation. The cold background radiant brightness temperature is about 2.73 K. The high-temperature point is provided by the spaceborne hot radiation calibration source. The source's radiant brightness temperature is approximately its physical temperature, about 300K. The physical temperature of the source was measured by a high-precision temperature measuring circuit.

Due to the characteristics of the semiconductor equipment used in the detector, the output voltage and input power of the radiometer deviate from the ideal linear relationship. In real applications, the microwave radiometer system is nonlinear, resulting in measurement errors. The larger the nonlinear coefficient, the greater the magnitude of the error. This nonlinear behavior requires as much as possible linearity improvement of the receiver during the design and manufacture of the instrument; the receiver should also work in the linear region. The microwave radiometer calibration results of the Fengyun-3 satellite show that the linearity of the receiver of the microwave radiometer needs to be larger than 0.9999, which is technically challenging in its implementation.

To improve the calibration accuracy, the measurement error caused by the receiver's nonlinearity must be taken into account, which requires a correction of the two-point calibration equation. Specifically, a quadratic term needs to be introduced to the two-point calibration equation to compensate for this nonlinearity. Therefore, the brightness temperature (T_B) of the target radiation is modified to

$$T_B = a_0 + a_1 V_O + a_2 V_O^{\,2} \tag{3}$$

where a_0, a_1, and a_2 are the scaling coefficients for each term, respectively, and V_O is the numeric value of the voltage when sensing the target.

2.2 Reflector Antenna

Errors in the brightness temperature estimation of the high and low-temperature references in the calibration method affect the accuracy of the linear calibration equation, thereby reducing the radiometer calibration accuracy. The two main factors inducing the error in estimating the brightness temperature of the cold and heat sources are the influence of the antenna sidelobe and the uncertainty in the measurement of the cold and heat calibration sources [14,15].

Microwave radiometers are divided into two categories based on the different antenna structures:

(1) mechanically scanning offset parabolic reflector antenna radiometers with shields, such as microwave thermometers and microwave hygrometers on the Fengyun-3 satellite;

(2) conically scanning offset parabolic reflector large-aperture antenna radiometers without shields, such as the microwave imager on the Fengyun-3 satellite. The different antenna structure results in different factors influencing the calibration error introduced by the antenna sidelobe.

The hot radiation calibration and the cold radiation calibration sources were used as the high- and low-temperature references in the ground vacuum calibration for the two-point calibration. The shielding cover was used for isolation to reduce the influence of stray background radiation. The shielding cover also emits radiation, which needs to be compensated for, based on its temperature. After the satellite is in orbit, the hot radiation calibration source and cold cosmic radiation were used as the high- and low-temperature references for the on-orbit two-point radiometer calibration.

The difference in antenna structure and the difference between the high- and low-temperature references in ground calibration and on-orbit calibration should be considered when examining the impact of the calibration source temperature measurement error on calibration accuracy.

Previous studies [16,17] have shown that a microwave radiometer needs to be equipped with an antenna of 5m diameter on a 36000km geostationary orbit satellite to meet the spatial resolution requirements for a radiometer in geostationary orbit and sense the atmosphere. A 5m aperture antenna system was developed. The electrical size of the antenna's main reflecting surface reached 7000 times its wavelength. The temperature range of the stationary orbit varied significantly, from -150℃ to about120℃. The manufacturing process of the antenna reflecting surface, thermal deformation, and antenna sidelobes impact the measurement results. The measurement error caused by the antenna sidelobe was estimated as follows.

The microwave radiometer is a passive detector. Its resolution relies on the shape of the antenna radiation pattern, $F_n(\theta,\phi)$. The ideal antenna is an antenna with a narrow pencil beam and no sidelobes. Besides the radiation energy received through the main antenna lobe, the antenna also receives other radiation through the rest of the radiation pattern. The power received by the microwave radiometer antenna is divided into two parts for estimating undesired contributions. One part is the contribution of the main lobe, and the other part is the contribution received from various directions other than the main lobe:

$$T_A = \frac{\iint\limits_{\mathrm{ML}} T_{AP}(\theta,\phi)F_n(\theta,\phi)d\Omega}{\iint\limits_{4\pi} F_n(\theta,\phi)d\Omega} + \frac{\iint\limits_{4\pi-\mathrm{ML}} T_{AP}(\theta,\phi)F_n(\theta,\phi)d\Omega}{\iint\limits_{4\pi} F_n(\theta,\phi)d\Omega} \tag{4}$$

where T_A is the apparent temperature of the radiation measurement of the microwave radiometer antenna. $T_{AP}(\theta,\phi)$ represents the apparent temperature distribution of the antenna orifice interface. For concise terminology, the second term in Equation (4) is called the contribution of the sidelobe.

The effective apparent temperature contributed by the main lobe is defined as:

$$\overline{T}_{ML} = \frac{\iint\limits_{\mathrm{ML}} T_{AP}(\theta,\phi)F_n(\theta,\phi)d\Omega}{\iint\limits_{ML} F_n(\theta,\phi)d\Omega} \tag{5}$$

where the integrals in the numerator and denominator of Equation (5) are evaluated on the solid angle of the main lobe of the antenna radiation pattern. According to the antenna principle, the main beam efficiency η_M is:

$$\eta_M = \frac{\iint\limits_{ML} F_n(\theta,\phi)d\Omega}{\iint\limits_{4\pi} F_n(\theta,\phi)d\Omega} \tag{6}$$

The product $\eta_M \overline{T}_{ML}$ is equivalent to the first term in Equation (4). Similarly, the second term in Equation (4) is equivalent to the product $\eta_m \overline{T}_{ML}$, where η_m is the antenna spurious factor:

$$\eta_m = \frac{\iint\limits_{4\pi-\mathrm{ML}} F_n(\theta,\phi)d\Omega}{\iint\limits_{4\pi} F_n(\theta,\phi)d\Omega} = 1-\eta_M \tag{7}$$

$\overline{T}_{SL}$ is defined as the effective apparent temperature contributed by the sidelobe. With the exception that the integral range is 4π minus the solid angle of the main lobe, the expression of $\overline{T}_{SL}$ is consistent with Equation (4).

$$\overline{T}_{SL} = \frac{\iint\limits_{4\pi - \Omega_M} T_{AP}(\theta,\phi) F_n(\theta,\phi) d\Omega}{\iint\limits_{4\pi - \Omega_M} F_n(\theta,\phi) d\Omega} \tag{8}$$

Using these new definitions, Equation (4) becomes

$$T_A = \eta_M \overline{T}_{ML} + (1-\eta_M)\overline{T}_{SL} \tag{9}$$

Due to the existence of antenna sidelobes, as shown in Fig. 2, the microwave radiometer is affected by stray radiation in the process of cold and hot calibration and ground observation, resulting in calibration errors.

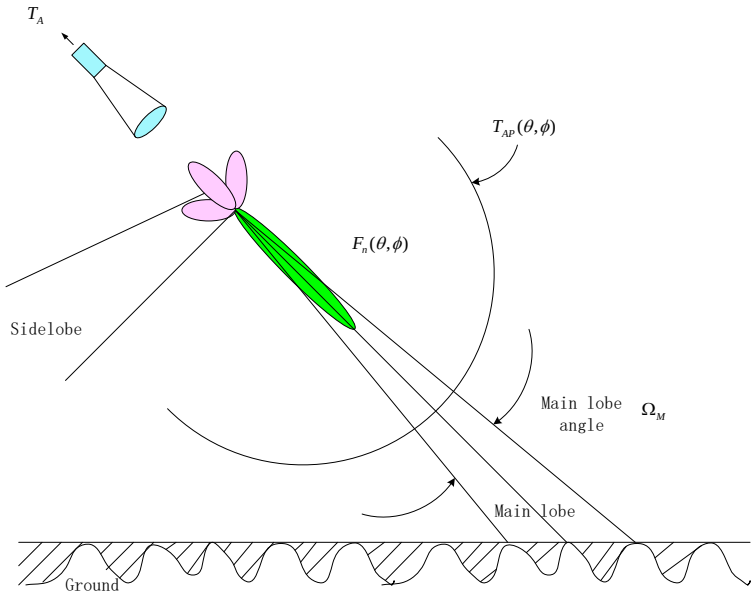

Fig 2: The contribution of the main lobe and sidelobes to the antenna temperature

However, in practical applications, it is impossible to know the temperature of the target relative to the antenna sidelobe. Therefore, a normally distributed random noise was used to correct for the temperature effect from the sidelobe, that is

$$\tilde{T}_A = T_A + n \tag{10}$$

where $n \sim N(0, \delta_n^2)$.

3.Piecewise Linear Model and its Estimation

3.1 Piecewise linear model

Due to various nonlinear factors in the microwave radiometer [18-20]

measurement process, the curve of output voltage versus temperature to be measured is usually a higher-order curve, as shown in Fig 3. In this case, it is challenging to perfectly fit the data regardless of whether a first-order or second-order model is used.

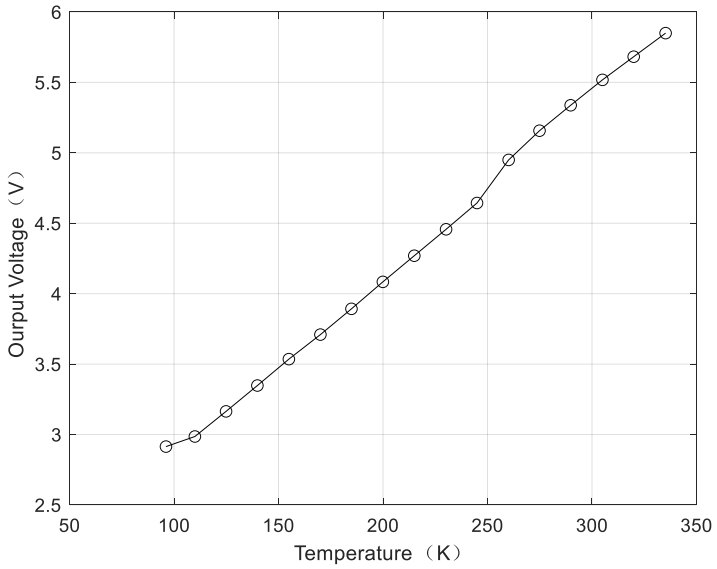

Fig 3: The relationship between the output voltage and temperature for the 183GHz microwave radiometer

Therefore, a piecewise linear model was introduced in this study to improve the accuracy of curve fitting and reduce model fitting errors. The system equations of the piecewise linear calibration are expressed as follows.

$$T_B = \begin{cases} a_0 \times V_O + b_0 + n & , V_{TH_0} \le V_O < V_{TH_1} \\ a_1 \times V_O + b_1 + n & , V_{TH_1} \le V_O < V_{TH_2} \\ \cdots & , \quad \cdots \\ a_{n-1} \times V_O + b_{n-1} + n & , V_{TH_{n-1}} \le V_O < V_{TH_n} \end{cases} \tag{111}$$

Where a_i, b_i are the system parameters for each linear segment. n stands for Gaussian white noise, which satisfies $n \sim N(0, \delta_n^2)$. In each linear segment of the piecewise calibration scheme, the radiation brightness temperature of the feed interface, the hot calibration source, and the cold cosmic radiation signal are the measurement values that can be calculated by the traditional two- point calibration method.

It should be emphasized that in the piecewise linear model, it is assumed

that the temperature-voltage curve is a monotonic function. This assumption has also been applied to the linear and quadratic system models.

3.2 Parameter estimation method

The system parameters a_i, b_i corresponding to each segment were determined in the piecewise linear system expressed by Equation (11). For the i-th linear segment:

$$T_B = a_i \times V_O + b_i + n \tag{112}$$

In the calibration process, the target temperature is known, and the output voltage of the receiver was measured.

$$\begin{aligned} V_O &= \alpha_i T_B + \beta_i + \tilde{n}, \\ \alpha_i &= 1/a_i \\ \beta_i &= -b_i / a_i \\ \tilde{n} &= -n / a_i \end{aligned} \tag{113}$$

The measurement results of the voltage at both segment ends follow Equation (14)

$$\begin{bmatrix} V_{OL} \\ V_{OH} \end{bmatrix} = \begin{bmatrix} T_{BL} & 1 \\ T_{BH} & 1 \end{bmatrix} \begin{bmatrix} \alpha_i \\ \beta_i \end{bmatrix} + \begin{bmatrix} \tilde{n}_L \\ \tilde{n}_H \end{bmatrix} \tag{114}$$

Equation (14) was rewritten as

$$\mathbf{V} = \mathbf{T}\Lambda + \tilde{\mathbf{n}} \tag{115}$$

In the linear system expressed by Equation (15), we used the least-squares method to estimate the parameters and obtained:

$$\hat{\Lambda} = (\mathbf{T}^H \mathbf{T})^{-1} \mathbf{T}^H \mathbf{V} \tag{116}$$

where $\hat{\Lambda} = [\hat{\alpha}_i, \hat{\beta}_i]^H$. $\hat{\alpha}_i$ and $\hat{\beta}_i$ are the least-squares estimates of α_i and β_i ,respectively.

The mean of the estimation error is:

$$\begin{aligned} E\{\Lambda - \hat{\Lambda}\} &= E\{(\mathbf{T}^H \mathbf{T})^{-1} \mathbf{T}^H \tilde{\mathbf{n}}\} \\ &= 0 \end{aligned} \tag{117}$$

Therefore, $\hat{\alpha}_i$ and $\hat{\beta}_i$ are unbiased estimates of α_i and β_i . The mean square error (MSE) of the estimation error is expressed as:

$$\begin{aligned} MSE &= Trace\{E\{(\Lambda - \hat{\Lambda})(\Lambda - \hat{\Lambda})^H\} \\ &= \sigma_{\tilde{n}}{}^2 Trace\{(\mathbf{T}^H\mathbf{T})^{-1}\} \end{aligned} \tag{118}$$

4. Calibration and Results

The calibration was performed in a vacuum calibration chamber by using a receiver calibration system. The receiver calibration system (except for the rotating scanning drive controller), the cold calibration source, and the temperature-adjustable source were installed in the vacuum chamber. The rest of the equipment was installed outside the vacuum chamber, as shown in Fig 4.

The hot radiation source calibration and the temperature-adjustable source were set in a plane perpendicular to the beam emitting axis plane of the rotating scanning mirror. As the rotating scanning mirror rotates periodically, the cold radiation calibration source signal enters the quasi- optical feed through the cold calibration mirror and the rotating scanning mirror. The radiation signals of the hot radiation calibration source and the temperature-adjustable source directly enter the quasi-optical feeding network through the rotating scanning mirror and are received by the 54GHz and 183GHz receivers after frequency separation. The information unit combines the data collected by the receiver into frames and sends them to the test equipment for data processing.

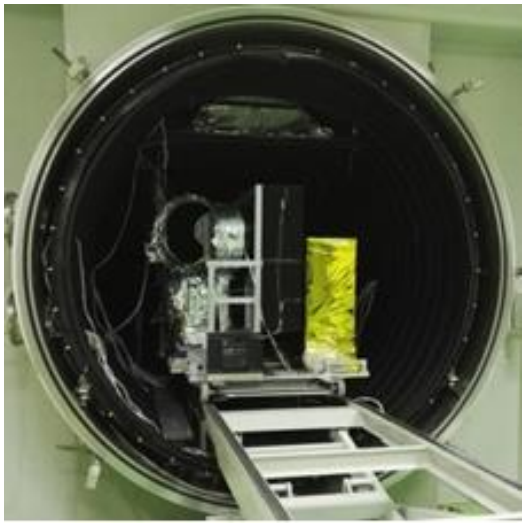

Fig 4: Picture of the installation of the vacuum microwave radiometer calibration system in the vacuum chamber

Table 1 shows the measured data of the 183GHz 1 channel. The linear model, quadratic model, and piecewise linear model were used for calibration using the 17 sets of collected data. The odd indexed data were used for parameter calculation. The even indexed data were back- plugged into the equations, i.e, the

target temperature obtained using the output voltage, and were compared with the collected data. The output voltage versus temperature results from the three models are shown in Fig 5. The figure shows large deviations from the measured results for both the linear model and the quadratic model. The piecewise linear model provides the best fit to the measured results with the smallest error.

Table 1

183GHz channel test data

Group	T_H **(K)**	T_C **(K)**	T_V **(K)**	V_H **(V)**	V_C **(V)**	V_V **(V)**
1	298.02	95.043	335.227	5.3988	2.9149	5.8497
2	298.01	95.035	319.956	5.4148	2.9256	5.6824
3	298.01	95.035	305.006	5.4316	2.9381	5.5179
4	298.01	95.035	289.794	5.4393	2.941	5.3376
5	298.003	95.043	274.896	5.4416	2.9404	5.1571
6	298.009	95.035	260.119	5.4167	2.917	4.9495
7	297.9857	95.01833	244.9871	5.29	2.806	4.6438
8	297.993	95.033	230.179	5.2857	2.8013	4.4569
9	297.991	95	214.974	5.2836	2.7992	4.2695
10	297.991	94.995	199.933	5.2808	2.7984	4.0838
11	297.99	95.047	184.909	5.2734	2.7927	3.8924
12	297.999	95.028	170.05	5.2736	2.7932	3.7096
13	297.99	95.137	154.964	5.2815	2.801	3.5353
14	297.989	95.133	139.897	5.2795	2.7985	3.3479
15	297.989	95.018	124.904	5.281	2.7992	3.1644
16	297.9686	95.015	109.9857	5.2873	2.8034	2.986
17	297.95	95.01	96.15714	5.4198	2.903	2.9144

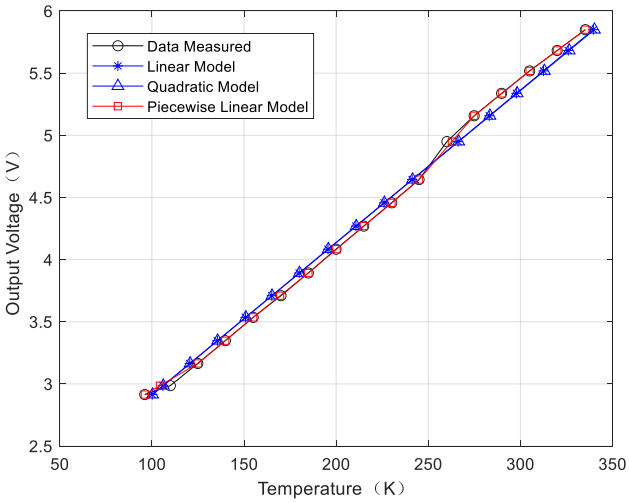

Fig 5: Test data processing results

In the curve described in the above figure, the parameters used by the linear model and quadratic model are to calculate the model parameters by using

the cold and hot temperature and output voltage of each calibration and average the model parameter results obtained from multiple calibration. After obtaining the model parameters, the target temperature is estimated by using the radiometer output voltage, and the obtained curve is depicted in the above figure. The piecewise linear model uses the odd index data in the measurement process for parameter calculation and uses the even index test data for back substitution (that is, infer the target temperature by using the output voltage and compare it with the measured results), and draws the curve in Fig. 6. It can be seen from the figure that there is a large deviation between the linear model and the quadratic model and the measured results. The piecewise linear piecewise model can better fit the measured results with the smallest error.

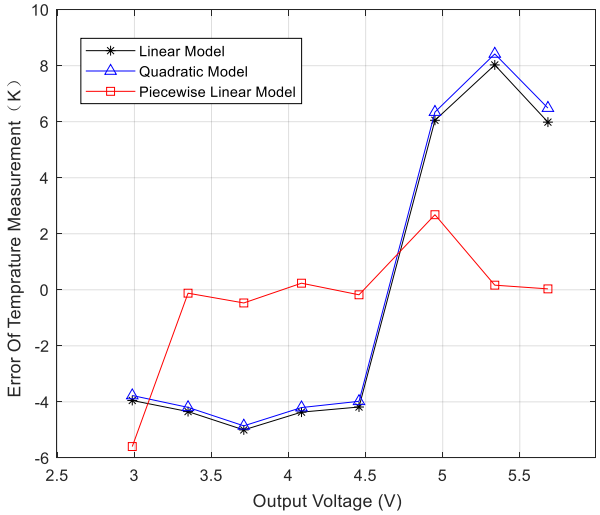

Fig 1: Relationship between radiometer output voltage and measured temperature error under different models

For the output value of the even index radiometer, the error between the estimated target temperature and the measured temperature under the three models is compared, as shown in the figure above. It can be seen from the figure that the piecewise linear model fits the nonlinear characteristics of the radiometer well and has the minimum estimation error.

5. Conclusions

In this study, the influence of the sidelobes of the antenna aperture and other uncertainty factors were taken into account during the model development process for the microwave radiometer calibration. A noise term was introduced into the model. A piecewise linear calibration method has been proposed to account for the nonlinear characteristics of the voltage-temperature curve

measured by the microwave radiometer. The least-squares method was used to estimate the parameters after introducing a noise term. The calibration results of the on-orbit microwave radiometer show that both the antenna aperture calibration and the feed interface calibration achieve satisfactory results. Since the antenna aperture calibration method has been used only recently, the advantages of the calibration using this method still need to be verified by more on- orbit calibration data.

R E F E R E N C E S

[1] Lu, N. Gu, S, The Status and Prospects of Atmospheric Microwave Sounding by Geostationary Meteorological Satellite. Advances in Met S&T. 2016, 6, 1, 120-123.

[2] Zhao, J. Zhang, D, Study on the Calibration of the Millimeter and Submillimeter Wave Radiometer. Radiometer. Remote Sensing Technology and Application. 2008, 23, 6, 717-720.

[3] Weng, F.; Zou, X.; Wang, X.; Yang, S.; Goldberg, M.D. Introduction to Suomi national polar-orbiting partnership advanced technology microwave sounder for numerical weather prediction and tropical cyclone applications. J Geophys Res: Atm 2012, 117, doi: ht t ps: // do i.o rg/ 10 .10 29 / 20 12 J D01 81 44 .

[4] Luan, H.; Zhao, K. Error analysis and accuracy validation of two-point calibration for microwave radiometer receiver. J Infrared Millim W 2007, 26, 289-292.

[5] Wang, Z.; Liu, J.; Zhang, Y.; Zheng, W.; Li, B. Calibration of Multiband Microwave Radiometer Used for Oceanic Calibration/Validation Site. Chinese J Space Sci 2014, 34, 474-482.

[6] An, D.; Gu, S.; Yang, Z.; Chen, W. On-orbit radiometric calibration for nonlinear of FY-3C MWTS. J Infrared Millim W 2016, 35, 317-321.

[7] Wu Y. et al. A review on geostationary earth orbit microwave atmospheric sounding technology. Remote Sensing for Land and Resources. 2017, 29, 4, 1- 5.

[8] Chen, W.; Liu, G.; He, J.; Pan, L. Research on the Method of Reducing the Receiver Non-Linear Deviation of the Microwave Radiation Imager. Remote Sens Technol Appl 2017, 32, 121-125.

[9] Wang, Z.; Li, J. Calibration Principle and Algorithm of Microwave Sounder Onboard Feng Yun-3 Satellites. Remote Sens Technol Appl 2019, 34, 1197-1204.

[10] Liu, G. Comparison and Research on Calibration Methods of Spaceborne Microwave Imaging Radiometer. J Microwaves 2012, S2, 440-442.

[11] Xie, Z.; Li, X.; Yao, C.; Jiang, L.; Li, X. Research on Geostationary Orbit Microwave Radiometer Technology. Aerospace Shanghai 2018, 35, 20-28.

[12] Ulaby, F.T.; Moore, R.K.; Fung, A.K. Microwave Remote Sensing - Active and Passive - Volume I - Microwave Remote Sensing Fundamentals and Radiometry; Wesley Publishing Company: Addison, 1981.

[13] Ren, Y.; Yu, Y. Two-point calibration error analysis of microwave radiometer. Electronic Measurement Technology. 2020, 43, 24,48-51.

[14] Miao, J.; Liu, D. Introduction to Microwave Remote Sensing; Machinery Industry Press: Beijing, 2012.

[15] Yang, M.; Zhou, Y.; Zhang, L.; Han, C. Correction to Nonlinearity in Interferometric Data and Its Effect on Radiometric Calibration. Chinese J Lasers 2017, 44, 1-7.

[16] Wang, L.; Hu, Q.; Chen, L. Wide dynamic nonlinear radiometric calibration of optical satellite sensors using multiple stable earth targets. J Remote Sens 2017, 21, 892-906.

[17] Jiang, L.; Qiao, Y.; Wang, Y.; Sun, Y.; Yao, C. Measurement and Analysis on Sensitivity of Receiving and Calibration System of Space-Borne Microwave Radiometer. J Terahertz Sci Electr Inf Technol 2016, 14, 843-847.
[18] Gu, S.; Wang, Z.; Ma, G.; al., e. Meteorological satellite microwave atmospheric remote sensing; Science Press: Beijing, 2021.
[19] Huang, Q.; Xiao, Z.; Zhang, Z.; Guo, W. Millimeter Wave Radiometer Calibration System. J Infrared Millim W 2003, 22, 119-122.
[20] Nian, F.; Yang, Y.; Wang, W.; Huang, P. Research on Microwave and Millimeter Wave Radiometer Wideband Brightness Temperature Calibration System. Sys Eng Electr 2011, 33, 750-754,810.